Research Article

Reconstitution of an anti-HER2 antibody paratope by grafting dual CDR-derived peptides onto a small protein scaffold

Kyra See, Tetsuya Kadonosono, Yumi Ota, Kotaro Miyamoto, Wanaporn Yimchuen, and Shinae Kizaka-Kondoh

School of Life Science and Technology, Tokyo Institute of Technology, Yokohama 226-8501, Japan

Correspondence: Tetsuya Kadonosono, School of Life Science and Technology, Tokyo Institute of Technology, Yokohama 226-8501, Japan.

E-mail: tetsuyak@bio.titech.ac.jp

Keywords:

Complementarity-determining region grafting, computational screening, monoclonal antibody, paratope, target-binding peptide

Abbreviations: CDR, complementarity-determining region; **FLAP,** fluctuation-regulated affinity protein; **FN3,** fibronectin type III domain; **HER2,** human epithelial growth factor receptor type 2; **mAb,** monoclonal antibody; **MD,** molecular dynamics; **MM/GBSA,** molecular mechanics/generalized Born surface area; **RMSF,** root-mean-square-fluctuation; **RSMD,** root-mean-square-deviation

This article has been accepted for publication and undergone full peer review but has not been through the copyediting, typesetting, pagination and proofreading process, which may lead to differences between this version and the <u>Version of Record</u>. Please cite this article as <u>doi:</u> 10.10002/biot.202000078.

Abstract

Target-binding small proteins are promising alternatives to conventional monoclonal antibodies (mAbs), offering advantages in terms of tissue penetration and manufacturing costs. Recently, we developed a design strategy to create small proteins called fluctuation-regulated affinity proteins (FLAPs) consisting of a structurally immobilized peptide from the complementarity-determining region (CDR) loops of mAbs (CDR-derived peptide) and a protein scaffold. Because mAb paratopes are usually composed of multiple CDRs, FLAPs with multiple binding peptides may have an enhanced target-binding capability. Here, we describe a strategy to create FLAPs bearing dual CDR-derived peptides (D-FLAPs) using the anti-human epithelial growth factor receptor type 2 (HER2) mAb trastuzumab as a basis. Computationally selected CDR-derived peptides were first grafted onto two adjacent loops of the fibronectin type III domain (FN3) scaffold, yielding 80 D-FLAP candidates. After computational screening based on their similarity to the parental mAb with regard to the conformation of paratope residues, two candidates were selected. After further evaluation with ELISA, one D-FLAP with HYTTPP and GDGFYA peptides from CDR-L3 and CDR-H3 of the parental mAb, respectively, was found to bind HER2 with a dissociation constant of 58 nM. Our method applies to various mAb drugs and allows the rational design of small protein alternatives.

1 Introduction

Monoclonal antibodies (mAbs) target a wide range of disorders, including cancer and inflammatory diseases [1]. Their effectiveness is attributed to their unprecedentedly high affinity and specificity for their targets, which are mediated by paratopes consisting of amino acid residues across six complementarity-determining regions (CDRs) in the heavy (CDR-H1–H3) and light (CDR-L1–L3) chains [2]. However, several challenges have been recognized in the therapeutic application of mAbs, including insufficient penetration into solid tumors [3,4] and prohibitive treatment costs [5,6].

Target-binding small proteins have emerged as viable alternatives to mAbs. With a small molecular weight (2–20 kDa), they have several advantages over mAbs in terms of tissue penetration and manufacturing requirements [7]. These proteins are often composed of a small protein scaffold that confers conformational stability and one or more surface-exposed loops that facilitate target binding [7]. The standard method to develop target-binding small proteins involves the creation of a large protein library, which consists of mutant scaffold proteins with amino acid sequence-randomized loops, followed by *in vitro* or *in vivo* selection of target binders [8]. An alternative and emerging approach is grafting CDRs onto small protein scaffolds. The technique of CDR grafting was originally used for mAb humanization through reconstitution of the original non-human mAb paratope on a human mAb framework [9]. Following the same principle, a general strategy for reconstitution of mAb paratopes on small protein scaffolds through CDR grafting may make it possible to more efficiently create target-binding small proteins with the same epitopes as those of the parental mAbs.

A leading example of success is the development of lysozyme-binding small proteins by grafting CDRs from camelid single domain antibodies or nanobodies, which have three CDRs (CDR-1–3), onto small protein scaffolds [10-12]. Because CDR-3 of lysozyme-binding nanobodies serves as the primary point of target binding [13] and fits concave epitopes such as deep pockets [14], grafting of a single CDR-3 is sufficient to transfer the original paratope to a small protein scaffold. However, the creation of target-binding proteins from nanobody-derived CDRs has been met with limited success [11,12]. An alternative approach is to use mAb-derived CDRs. Since antibody paratopes are usually formed by a combination of dominant and ancillary CDRs [15-17] that bind to linear or planar epitopes [14], optimal paratope reconstitution is difficult with a single CDR graft onto a small protein scaffold. However, grafting multiple CDR

peptides onto a small protein scaffold is challenging. To date, there have been no reports that describe such an undertaking.

In this study, we sought to confront this problem and succeeded in obtaining a small protein with two CDR-derived peptides that conformationally mimic the parental antibody paratope. Recently, we reported a computational design strategy to develop target-binding small proteins called fluctuation-regulated affinity proteins (FLAPs). These FLAPs have a structurally immobilized single CDR-derived peptide [15] or target-binding peptide [18] to reduce entropic energy loss upon target binding. Based on the same concept, in this study, we describe the computational design of FLAPs bearing dual CDR-derived peptides (D-FLAPs). We designed and screened a human epithelial growth factor receptor type 2 (HER2)-binding D-FLAP with dual CDR-derived peptides from the anti-HER2 mAb trastuzumab immobilized on a fibronectin type III domain (FN3) scaffold. The selected D-FLAP, which had HYTTPP and GDGFYA peptides from CDR-L3 and CDR-H3 of trastuzumab, respectively, bound to HER2 with a dissociation constant (K_D) of 58 nM. Furthermore, additional simulations and binding energy calculations suggested that the grafted CDR peptides were indeed important for binding to HER2. This study is the first example of multiple CDR grafting from a mAb onto a small protein scaffold and may serve as a foundation for the development of therapeutically applicable targetbinding small proteins from mAbs.

2 Materials and methods

2.1 Molecular dynamics (MD) simulations

The initial coordinates of the trastuzumab Fab-HER2 complex and FN3 structures were obtained from Protein Data Bank (PDB) accession codes 1N8Z and 1TTG, respectively. The structures of FN3 with CDR-derived peptides (D-FLAP candidates) were generated by introducing point mutations into the FN3 structure. All MD simulations were performed using the AMBER 16 program package [19] on TSUBAME (Global Scientific Information and Computing Center, Tokyo Institute of Technology).

For binding free energy calculations using the trastuzumab Fab-HER2 complex, the systems were fully solvated with explicit solvent and 2 Na+ counterions were added to obtain electrostatic neutrality. We employed the AMBER ff14SB force field for proteins and the TIP3P model for water molecules. The systems were optimized by energy minimization and

equilibrated with backbone restraints. Production runs were then performed for 100 ns. The binding free energy of the trastuzumab Fab and HER2 during the final 50 ns of the production run was calculated using the molecular mechanics/generalized Born surface area (MM/GBSA) module.

To predict the structures and molecular dynamics of D-FLAP candidates, production runs were performed for 100 ns for trajectory analysis. The AMBER ff14SB force field and GB/SA implicit solvent model were used. The time-step for MD simulations was set to 2 fs with the SHAKE algorithm. A non-bonded cutoff of 999.9 Å was used. The temperature was kept constant at 300 K using the Berendsen rescaling method. The root-mean-square fluctuation (RMSF) values during the final 10 ns of each production run were calculated to investigate the backbone fluctuations in each system using the cpptraj module. Similarly, the conformational similarity of HER2-binding residues between the trastuzumab Fab and FN3 mutants during the final 10 ns of each production run was evaluated by calculating the root-mean-square deviation (RMSD) values using the cpptraj module.

Docking simulations were performed using RosettaDock 4.0 [20]. First, local all-atom protein-protein docking was carried out, generating 3,000 complex models. Structural clustering analysis was then performed on the 200 lowest interface energy-scoring models to identify commonly occurring poses. The lowest energy model from this analysis was used as the initial structure for local refinement docking to further optimize the energy of the docked complex, producing 1,000 models. Finally, interface energy (energy at the interface between D-FLAP models and HER2 target) was plotted against interface RMSD (RMSD between D-FLAP models and initial structure).

For binding free energy calculations using the D-FLAP-HER2 complex, docking models from the three lowest energy clusters obtained after structural clustering analysis were used. The AMBER ff14SB force field and GB/SA implicit solvent model were used. The time-step for MD simulations was set to 2 fs with the SHAKE algorithm. A non-bonded cutoff of 999.9 Å was used. The temperature was kept constant at 300 K using the Berendsen rescaling method. The systems were optimized by energy minimization and equilibrated with backbone restraints. Production runs were then performed for 100 ns. The binding free energy of D-FLAP and HER2 during the final 10 ns of production run was calculated using the MM/GBSA module. For all MM/GBSA calculations, the generalized Born method developed by Onufriev and colleagues

(igb=5) was used [21]. Salt concentration, surface tension, and rgbmax, or the maximum distance between atom pairs to be considered during the calculation, were all set to default (saltcon=0.0, surften=0.0072, and rgbmax=25.0, respectively). The final 10 ns of each production run was also used for the calculation of RMSD values between the three models and the trastuzumab Fab using the cpptraj module.

2.2 Plasmid construction and protein purification

Recombinant DNA experiments were carried out according to the Tokyo Institute of Technology recombinant DNA experimental safety management regulations defined by the Tokyo Institute of Technology recombinant DNA experimental safety management committee. cDNA encoding the fusion protein consisting of wild-type FN3, a GGGS linker, and His-tag (FN3) was inserted into the multiple cloning site of the pGEX-6P-3 plasmid (GE Healthcare, Little Chalfont, UK). cDNA constructs encoding the FN3 mutants (FN3-L, FN3-H, FN3.38, and D-FLAP) were prepared by site-directed mutagenesis using the previously constructed FN3 cDNA as the template. *E. coli* BL21 (DE3) pLysS cells (Promega, Fitchburg, WI, USA) or *E. coli* Shuffle® T7 Express cells (New England BioLabs, Ipswich, MA, USA) were transformed with the plasmid vectors expressing FN3 and FN3 mutants. For enzyme-linked immunosorbent assays (ELISAs), the GST- and His-tagged FN3 and FN3 mutant proteins were expressed and purified from the supernatants of bacterial extracts using glutathione agarose beads (Sigma-Aldrich, St. Louis, MO, USA) and a HisTrap HP column (GE Healthcare) with an AKTA pure 25 system.

2.3 ELISA

ELISAs were carried out in 96-well black plates (Thermo Fisher Scientific, Waltham, MA, USA) with all steps performed at room temperature except coating that was conducted by incubation with HER2-Fc ($50 \text{ ng}/50 \mu\text{L PBS}$) overnight at 4°C Blocking was performed with 2% Perfect Block (MoBiTec, Göttingen, Germany) in PBS (PBS-PB) for 2 h, followed by washing three times with 0.05% Tween-20 in PBS (PBS-T) and incubation with FN3-L, FN3-H, or D-FLAP in PBS-PB for 1 h. The wells were then washed again three times with PBS-T and incubated with a 1000-fold diluted HRP-conjugated anti-His-tag antibody (Abcam, Cambridge, MA, USA) in PBS-PB for 1 h. Before detection using the QuantaRed Enhanced Chemifluorescent HRP Substrate kit (Thermo Fisher Scientific), the wells were first washed three times with PBS-T and then another three times with PBS. The resulting fluorescence signals were measured using an Infinite F500 plate reader (Tecan, Mannedorf, Switzerland) with specific filters (Ex/Em = 535 nm/590 nm).

3 Results

3.1 Selection of CDR-derived peptides

The basic design concept of FLAPs, in which single CDR-derived peptides are structurally immobilized by grafting onto small protein scaffolds, led us to hypothesize that the paratope of mAbs could be reconstituted by immobilizing multiple CDR-derived peptides within the same scaffold (Figure 1A). To test the hypothesis, we first identified CDR-derived peptides that comprise the paratope of the anti-HER2 mAb trastuzumab. HER2 was chosen as the target because of the availability of the structural data of the trastuzumab-HER2 complex [22] and the status of HER2 as a well-established molecular target for breast cancer [23]. After calculation of the binding free energy of each residue, four (F53, Y92, T93, and T94) and six (R50, Y57, R59, R98, F104, and Y105) residues from the light and heavy chains of trastuzumab, respectively, were identified as HER2-binding residues with calculated binding free energy values of less than -2 kcal/mol (Figure 1B). Among them, Y92, T93, and T94 (YTT) residues in CDR-L3 and F104 and Y105 (FY) residues in CDR-H3 were found at loop regions, while the other residues were located on β -sheet structures (Figure 1C). Therefore, we used CDR-derived peptides containing these five residues for grafting.

3.2 Grafting of CDR-derived peptides onto an FN3 scaffold

FN3 exhibits many properties of an ideal protein scaffold, such as a small molecular size (10 kDa), high stability, high solubility, and high tolerance to mutations. Furthermore, its structural similarity to the mAb immunoglobulin domain [24] makes it a suitable scaffold for mAb-derived CDR grafting. To graft CDR-derived peptides, we selected two loops of FN3, 21-SWDAPAVTVR-30 (loop A) and 51-PGSKST-56 (loop B), because their proximity and anti-parallel structure were similar to those of CDR-L3 and CDR-H3 in trastuzumab (Figure 2A). In a previous study, we found that in 99% of mAb light chains and 93% of mAb heavy chains, the longest contiguous sequence of antigen-contact residues was six amino acids [15]. Therefore, we prepared continuous peptides with six amino acids each that contain HER2-binding residues L3.1–L3.4 and H3.1–H3.4 from CDR-L3 and CDR-H3, respectively (Table 1) and grafted them into loops A.1–A.5 and B.1, respectively (Figure 2B), for a total of 80 D-FLAP candidates (FN3.1–FN3.80).

3.3 Identification of a D-FLAP with a reconstituted HER2-binding surface

The structures of FN3.1–FN3.80 predicted by MD simulations were screened to identify a D-FLAP with the reconstituted paratope of trastuzumab. First, the fluctuation of the five HER2-

binding residues in each loop was evaluated based on the RMSF values of all hydrogen-free atoms calculated using the trajectories of MD simulations. A previously determined threshold of RMSF < 1.5 Å was used to evaluate the structural immobilization of peptides, because structural immobilization was generally found to yield higher binding affinities in a previous study [15]. These calculations revealed that the average RMSF values of both the YTT and FY residues of all candidates and the trastuzumab Fab were <1.5 Å (Figure 3A), indicating that these residues were structurally immobilized on both trastuzumab and the FN3 scaffold. Then, the conformational similarity of the HER2-binding residues in each candidate to the corresponding residues in the antigen-free and antigen-bound structures of the trastuzumab Fab (i.e., the structure of the trastuzumab Fab extracted from the original trastuzumab-HER2 complex, alone and with its target molecule HER2, respectively) was evaluated using the RMSD values of the five Cα atoms, which were calculated using structures generated after 100-ns MD simulations (Figure 3B). As expected, the RMSD value between the antigen-free and antigen-bound states of the trastuzumab Fab was small (1.01 Å) considering that the residues on the original trastuzumab Fab were structurally immobilized. Among the 80 candidates, we found two candidates, FN3.38 (23-QHYTTP-28 and 51-GDGFYA-56) and FN3.58 (24-HYTTPP-29 and 51-GDGFYA-56), which had RMSD values of <2 Å between both antigen-free and antigen-bound states of the trastuzumab Fab. The structural comparison also showed that both FN3.38 and FN3.58 had HER2-binding surfaces similar to that of the trastuzumab Fab (Figure 3C).

3.4 Evaluation of D-FLAP binding to HER2

Recombinant FN3.38 and FN3.58 proteins were expressed using a bacterial system and purified by affinity chromatography, after which their affinity toward HER2 was determined. Because FN3.38 had a lower binding affinity for HER2 in comparison to that of FN3.58 when evaluated by ELISA (K_D values of 380 and 58 nM, respectively) (Figure 4A), we decided to further characterize FN3.58 (hereafter referred to as D-FLAP). To evaluate the effect of dual CDR grafting, FN3 mutants harboring single CDR-derived peptides FN3-L (24-HYTTPP-29) and FN3-H (51-GDGFYA-56) were also prepared. Measurement of affinity for HER2 by ELISA revealed that D-FLAP, FN3-L, and FN3-H bound to HER2 with K_D of 58, 3700, and 620 nM, respectively, suggesting that both CDR-derived peptides in D-FLAP contributed cooperatively to target binding (Figure 4A). As expected, wild-type FN3 showed no apparent binding to HER2. These results support the validity of the rationale behind our design.

To further investigate the binding of D-FLAP to HER2, we first performed protein docking simulations. Analysis of the docking energy landscape yielded a binding funnel converging toward the lowest energy structure (Figure 4B), suggesting that the docking simulations were able to successfully produce low-energy models. In the three lowest energy models, the loops containing the grafted CDR sequences appeared to be most proximal to HER2, suggesting that target binding was mediated by these loops (Figure 4C). Using these models, we then performed MM/GBSA binding free energy calculations coupled with per-residue decomposition to determine the contribution of each residue to HER2 binding (Figure 4D). The binding energy values of the segment containing the heavy chain CDR-derived peptide were more negative than those of other residues comprising the FN3 scaffold for all three models, suggesting that this peptide was critical for HER2 binding. In particular, the 54-FY-55 residues, which were initially identified and used as the basis for CDR-derived peptide selection, exhibited greater negative values than nearby residues, supporting the approach to identify CDR residues important for target binding. In contrast, the peptide derived from the trastuzumab light chain exhibited negative binding values in only one model. Additionally, in that same model, the CDR-derived histidine residue (H24) on the same loop yielded a much greater negative binding energy value than the initially selected residues (25-YTT-27). As our in vitro results demonstrated the contribution of the light chain-derived peptide to target binding (Figure 4A), the difference in binding energy values may be due to the light chain CDR residues accommodating the change in the framework from IgG to FN3. This is in line with previous findings that light chain CDRs generally play a more secondary or supporting role in target binding, such as stabilization of other CDRs [15-17]. Finally, we calculated the RMSD values of the HER2-binding residues between the three models and the antigen-free and antigen-bound structures of trastuzumab Fab. The rank 1 model yielded RMSD values of 1.64 Å and 1.86 Å to the antigen-free and antigen-bound structures, respectively; rank 2, 1.73 Å and 2.00 Å; and rank 3, 1.74 Å and 2.10 Å. The small RMSD values associated with the top-ranked model further support our use of CDR grafting to achieve paratope reconstitution in D-FLAP. Overall, these results suggest that multiple CDR grafting from mAbs to small protein scaffolds is a promising strategy to develop target-binding small proteins from mAbs.

4 Discussion

In this study, we present a computational method to design and select dual CDR-grafted mimetics known as D-FLAPs. This method involves calculation of the binding free energy to select important target-binding residues, followed by a screening step that employs conformational similarity as the basis to select candidates for further investigation *in vitro*. This approach was used to screen 80 protein candidates generated by simultaneously grafting CDR sequences from CDR-L3 and CDR-H3 of the anti-HER2 mAb trastuzumab onto the FN3 scaffold to reconstitute the mAb paratope. The final candidate, D-FLAP, was found to bind to HER2 *in vitro*. Furthermore, the binding affinity of D-FLAP was superior to that of the corresponding single chain controls (Figure 4A), suggesting cooperative binding from both CDRs, which agrees with previous observations [16,17]. These results indicate that the design strategy described in this study can facilitate the development of small protein alternatives from currently available mAbs.

The scaffold used in this study, the FN3 protein, is often used in the design of targetbinding proteins due to its small size and high stability [24]. Antibody alternatives that are based on the FN3 protein scaffold are sometimes referred to as monobodies. There have been several reports regarding the development of these FN3-based antibody mimetics, with a wide range of targets including VEGFR-2 [25] and PD-L1 [26]. These monobodies were developed primarily using technologies such as phage display and mRNA display to select binders from libraries with randomized sequences in up to three loops present in the FN3 protein [27,28]. Our group has also succeeded in creating HER2-binding small proteins based on the FN3 protein scaffold through conventional phage display library screening and subsequent affinity maturation [18]. In this study, an FN3-based antibody mimetic was developed using an alternative approach that does not involve designing and creating libraries in vitro. The FN3 protein has structural similarity to the mAb immunoglobulin domain, making it an attractive candidate scaffold for mAb-derived CDR grafting because CDR peptides grafted onto the FN3 scaffold would be more likely to mimic their original conformation on the parental mAb. This is supported by findings from our recent study involving the grafting of single CDR peptides onto several scaffold proteins, which showed that the FN3 scaffold produced more target-binding mimetics than other scaffold proteins [15]. The current study builds on our previous work and improves upon them by demonstrating the following: 1) Computational design and selection of FN3 mutants bearing grafted CDR peptides can generate a target-binding mimetic on par with This article is protected by copyright. All rights reserved.

that obtained through conventional screening methods [18], and 2) the binding affinity of FN3 mutants bearing single CDR-derived peptides [15] can be improved using multiple CDR peptides (Figure 4A).

The goal of this study was to reconstitute the paratope of the mAb trastuzumab. However, the binding affinity of the D-FLAP developed using our strategy did not reach that of trastuzumab (K_D = 0.47 nM) [15]. Notably, although the grafted CDR residues were structurally immobilized, as indicated by their RMSF values (Figure 3A), most candidates exhibited RMSD values of >2 Å between the trastuzumab Fab (Figure 3B). Therefore, inadequate structural similarity between the designed D-FLAPs and parental mAb may be the primary reason for the lower binding affinity of D-FLAP than that of trastuzumab. To overcome this, a preliminary step to select scaffolds based on their structural similarity to the variable region of the parental mAb can be incorporated. Using scaffolds with high initial structural similarity to parental mAbs can lead to a better design of D-FLAP candidates with high binding affinities for their targets.

Previous findings from studies on CDR grafting for mAb humanization describe enhancements in binding affinity upon the addition of several critical framework residues considered to be important to maintain the conformation of CDR loops [29,30]. Indeed, the results from binding energy calculations performed on the trastuzumab Fab showed that several residues outside the CDR loops (i.e., in the framework region) also exhibited values of <- $^2 \, \text{kcal/mol}$ (Figure 1B). In particular, R50 from the VH domain of trastuzumab may be of interest because it has been previously found to form hydrogen bonds with HER2 despite being in the framework region [31]. Similarly, CDR residues with favorable binding energy values, such as Y57 and R98, may also improve binding affinity if used for grafting despite being located on β -sheets. In summary, the inclusion of other critical residues may lead to the design of D-FLAP candidates with improved structural similarity to the parental mAb as well as better binding affinities.

One limitation of performing screening computationally rather than through standard *in vitro* display library methods is that the use of ideal conditions (i.e., both the target and the respective binding protein are isolated) makes it difficult to account for selectivity and off-target binding. This also highlights the need to further characterize any peptides obtained from computational screening through additional experiments both *in vitro* and *in vivo*. However, *in vitro* and *in vivo* experiments are time-consuming and expensive. Therefore, better strategies to

connect computational screens that efficiently select reliable candidates to actual drug development are desired, and this study presents one such strategy.

In conclusion, our study describes the successful development of a D-FLAP that is the first example of an antibody mimetic created by grafting of multiple CDR-derived peptides onto a small protein scaffold. Our strategy provides a foundation for the development of high affinity target-binding small protein alternatives from existing mAbs, which have various applications in diagnostics and therapeutics.

Acknowledgments

We thank the Biomaterials Analysis Division, Open Facility Center, Tokyo Institute Technology for performing DNA sequence analyses. We thank Mitchell Arico from Edanz Group (https://enauthor-services.edanzgroup.com/) for editing a draft of this manuscript. This study was partially supported by JSPS KAKENHI, Grant Number JP19K06970 (to T.K.).

Conflict of interest

The authors declare no financial or commercial conflict of interest.

Data availability statement

The data that support the findings of this study are available from the corresponding author upon reasonable request.

5 References

- [1] M. S. Kinch, *Drug Discov. Today* **2015**, *20*, 393.
- [2] L. G. Presta, Curr. Opin. Biotechnol. 1992, 3, 394.
- [3] C. M. Lee, I. F. Tannock, *BMC Cancer* **2010**, *10*, 255.
- [4] G. M. Thurber, M. M. Schmidt, K. D. Wittrup, Adv. Drug Deliv. Rev. 2008, 60, 1421.
- [5] L. M. Weiner, Nat. Rev. Cancer 2007, 7, 701.
- [6] E. Sparrow, M. Friede, M. Sheikh, S. Torvaldsen, Bull. World Health Organ. 2017, 95, 235.
- [7] A. Skerra, Curr. Opin. Biotechnol. 2007, 18, 295.
- [8] A. R. Baloch, A. W. Baloch, B. J. Sutton, X. Zhang, Crit. Rev. Biotechnol. 2016, 36, 268.
- [9] J. R. Apgar, M. Mader, R. Agostinelli, S. Bernard, P. Bialek, M. Johnson, Y. Gao, M. Krebs, J. Owens, K. Parris, M. St Andre, K. Svenson, C. Morris, L. Tchistiakova, *mAbs* **2016**, *8*, 1302.
- [10] M. Nicaise, M. Valerio-Lepiniec, P. Minard, M. Desmadril, *Protein Sci.* **2004**, *13*, 1882.
- [11] H. Inoue, A. Iihara, H. Takahashi, I. Shimada, I. Ishida, Y. Maeda, *Protein Sci.* **2011**, *20*, 1971.
- [12] S. Pacheco, G. Béhar, M. Maillasson, B. Mouratou, F. Pecorari, *Protein Eng. Des. Sel.* **2014**, *27*, 431.
- [13] A. Desmyter, T. R. Transue, M. A. Ghahroudi, M. H. Thi, F. Poortmans, R. Hamers, S. Muyldermans, L. Wyns, *Nat. Struct. Biol.* **1996**, *3*, 803.
- [14] O. Y. Dmitriev, S. Lutsenko, S. Muyldermans, J. Biol. Chem. 2016, 291, 3767.
- [15] T. Kadonosono, W. Yimchuen, Y. Ota, K. See, T. Furuta, T. Shiozawa, M. Kitazawa, Y. Goto, A. Patil, T. Kuchimaru, S. Kizaka-Kondoh, *Sci. Rep.* **2020**, *10*, 891.
- [16] H. Persson, W. Ye, A. Wernimont, J. J. Adams, A. Koide, S. Koide, R. Lam, S. S. Sidhu, *J. Mol. Biol.* **2013**, *425*, 803.
- [17] D. Kuroda, H. Shirai, M. Kobori, H. Nakamura, *Proteins* **2009**, *75*, 139.

[18] W. Yimchuen, T. Kadonosono, Y. Ota, S. Sato, M. Kitazawa, T. Shiozawa, T. Kuchimaru, M. Taki, Y. Ito, H. Nakamura, S. Kizaka-Kondoh, *RSC Adv.* **2020**, *10*, 15154.

[19] D. A. Case, D. S. Cerutti, T. E. Cheatham, III, T. A. Darden, R. E. Duke, T. J. Giese, H. Gohlke, A. W. Goetz, D. Greene, N. Homeyer, S. Izadi, A. Kovalenko, T. S. Lee, S. LeGrand, P. Li, C. Lin, J. Liu, T. Luchko, R. Luo, D. Mermelstein, K. M. Merz, G. Monard, H. Nguyen, I. Omelyan, A. Onufriev, F. Pan, R. Qi, D. R. Roe, A. Roitberg, C. Sagui, C. L. Simmerling, W. M. Botello-Smith, J. Swails, R. C. Walker, J. Wang, R. M. Wolf, X. Wu, L. Xiao, D. M. York, P. A. Kollman, *AMBER 2017*, University of California, San Francisco, **2017**.

[20] N. A. Marze, S. S. R. Burman, W. Sheffler, J. J. Gray, *Bioinformatics* **2018**, *34*, 3461.

[21] A. Onufriev, D. Bashford, D. A. Case, Proteins 2004, 55, 383.

[22] H.-S. Cho, K. Mason, K. X. Ramyar, A. M. Stanley, S. B. Gabelli, D. W. Denney Jr, D. J. Leahy, *Nature* **2003**, *421*, 756.

[23] R. Nahta, D. Yu, M.-C. Hung, G. N. Hortobagyi, F. J. Esteva, Nat. Clin. Pract. Oncol. 2006, 3, 269

[24] A. Koide, C. W. Bailey, X. Huang, S. Koide, *J. Mol. Biol.* **1998**, *284*, 1141.

[25] R. Mamluk, I. M. Carvajal, B. A. Morse, H. Wong, J. Abramowitz, S. Aslanian, A.-C. Lim, J. Gokemeijer, M. J. Storek, J. Lee, M. Gosselin, M. C. Wright, R. T. Camphausen, J. Wang, Y. Chen, K. Miller, K. Sanders, S. Short, J. Sperinde, G. Prasad, S. Williams, R. Kerbel, J. Ebos, A. Mutsaers, J. D. Mendlein, A. S. Harris, E. S. Furfine, *MAbs* **2010**, *2*, 199.

[26] S. Ramakrishnan, A. Natarajan, C. T. Chan, P. S. Panesar, S. S. Gambhir, *Protein Eng. Des. Sel.* **2019**, *32*, 231.

[27] M. D. Diem, L. Hyun, F. Yi, R. Hippensteel, E. Kuhar, C. Lowenstein, E. J. Swift, K. T. O'Neil, S. A. Jacobs, *Protein Eng. Des. Sel.* **2014**, *27*, 419.

[28] P. G. Chandler, A. M. Buckle, *Cells* **2020**, *9*, 610.

[29] C. Queen, W. P. Schneider, H. E. Selick, P. W. Payne, N. F. Landolfi, J. F. Duncan, N. M. Avdalovic, M. Levitt, R. P. Junghans, T. A. Waldmann, *Proc. Natl. Acad. Sci. USA* **1989**, *86*, 10029.

[30] G. X. Luo, L. A. Kohlstaedt, C. H. Charles, E. Gorfain, I. Morantte, J. H. Williams, F. Fang, *J. Immunol. Methods* **2003**, *275*, 31.

[31] C. Magdelaine-Beuzelin, Q. Kaas, V. Wehbi, M. Ohresser, R. Jefferis, M.-P. Lefranc, H. Watier, *Crit. Rev. Oncol. Hematol.* **2007**, *64*, 210.

Table 1. Amino acid sequences of the grafted CDR-derived loops

Loops	Amino acid sequences	
L3.1	QQHYTT	
L3.2	QHYTTP	
L3.3	НҮТТРР	
L3.4	YTTPPT	
H3.1	GGDGFY	
Н3.2	GDGFYA	
Н3.3	DGFYAM	
Н3.4	GFYAMD	

Figure legends

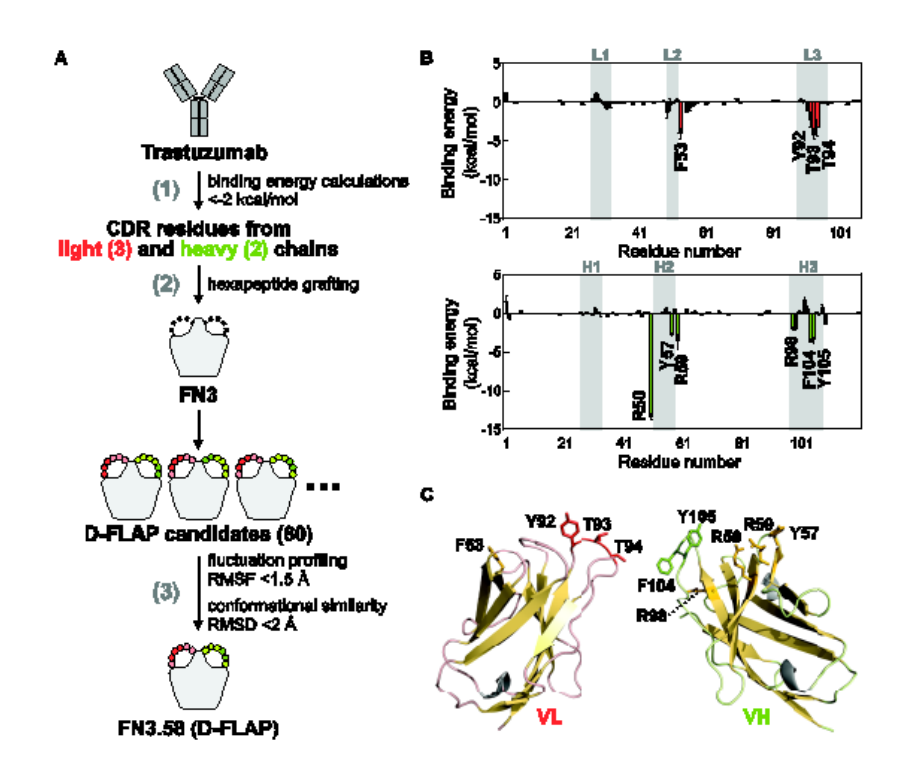


Figure 1. Selection of CDR-derived peptides for grafting. A) Overview of D-FLAP development by double CDR grafting for reconstitution of the trastuzumab paratope. (1) Binding energy calculations were used to select CDR residues from trastuzumab. (2) Hexapeptides containing these CDR residues were grafted onto two loops (dotted lines) of the FN3 scaffold, yielding 80 D-FLAP candidates. Red and green circles symbolize residues from VL and VH, respectively, with dark-colored circles representing HER2-binding residues. (3) Candidates were screened based on fluctuation and conformational similarity to the trastuzumab Fab. B) Identification of HER2-binding residues on the variable regions of trastuzumab light (VL) and heavy (VH) chains. The binding free energy of each residue to HER2 was calculated and shown as the mean ± SEM from 50 ns of the production run. Areas shaded in gray indicate the locations of CDR regions. C) Structures of trastuzumab VL and VH regions. Loops in the VL and VH regions are shown as pink and light green, respectively, and the positions of the HER2-binding residues selected using binding energy calculations are shown as red and green residues, respectively. β-Sheets and helices are shown as yellow and gray, respectively.

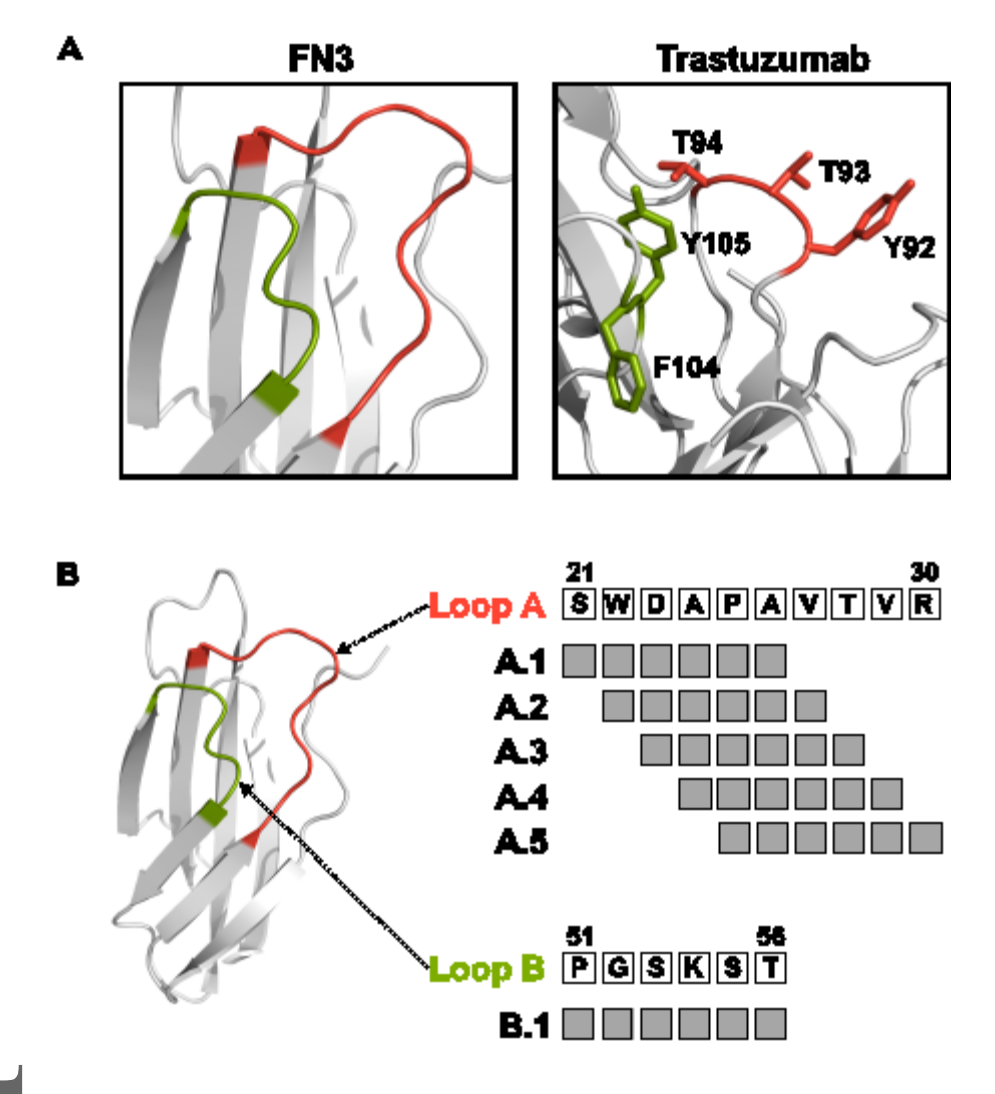


Figure 2. Grafting of CDR-derived peptides onto the FN3 scaffold. A) Structure of the loops used for grafting. FN3 had antiparallel loops A (red) and B (green) in close proximity, which resembled the conformation of the VL (red) and VH (green) HER2-binding residues depicted by the stick representation. B) Schematic diagram of the grafting sites in FN3. The amino acid residues of loops A and B are shown on each panel by one-letter notations in white boxes. The gray boxes to the right of A.1–A.5 and B.1 indicate the positions where Loop A and B amino acids were replaced by CDR-derived hexapeptides.

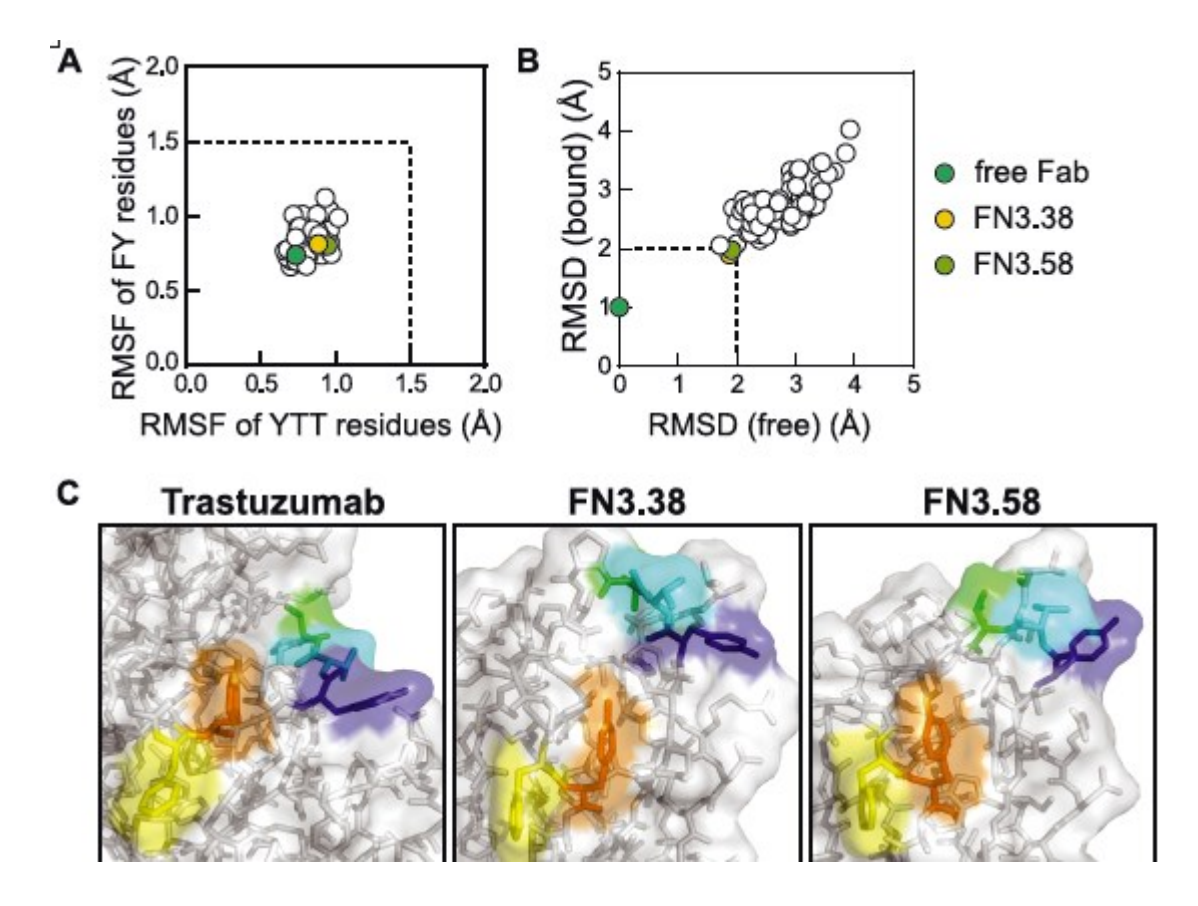


Figure 3. Assessment and screening of D-FLAP candidates. A) Profiling of fluctuation using RMSF calculations. The RMSF of the HER2-binding residues was calculated using hydrogen-free atoms from MD simulation trajectories. B) Screening of D-FLAP candidates by conformational similarity. The Cα atoms of the five HER2-binding residues generated after 100-ns MD simulations were used in calculations. The RMSD values of the candidates were then compared with those of the trastuzumab Fab in its antigen-free (free) and antigen-bound (bound) states. A and B) Shaded circles denote the antigen-free trastuzumab Fab (blue), FN3.38 (yellow), and FN3.58 (green). Data represent averages from three replicate simulations with random seeds. C) Side-by-side comparison of HER2-binding surfaces of the trastuzumab Fab, FN3.38, and FN3.58 (left to right). The HER2-binding residues are highlighted (F104, yellow; Y105, orange; Y92, blue; T93, cyan; T94, green).

٦

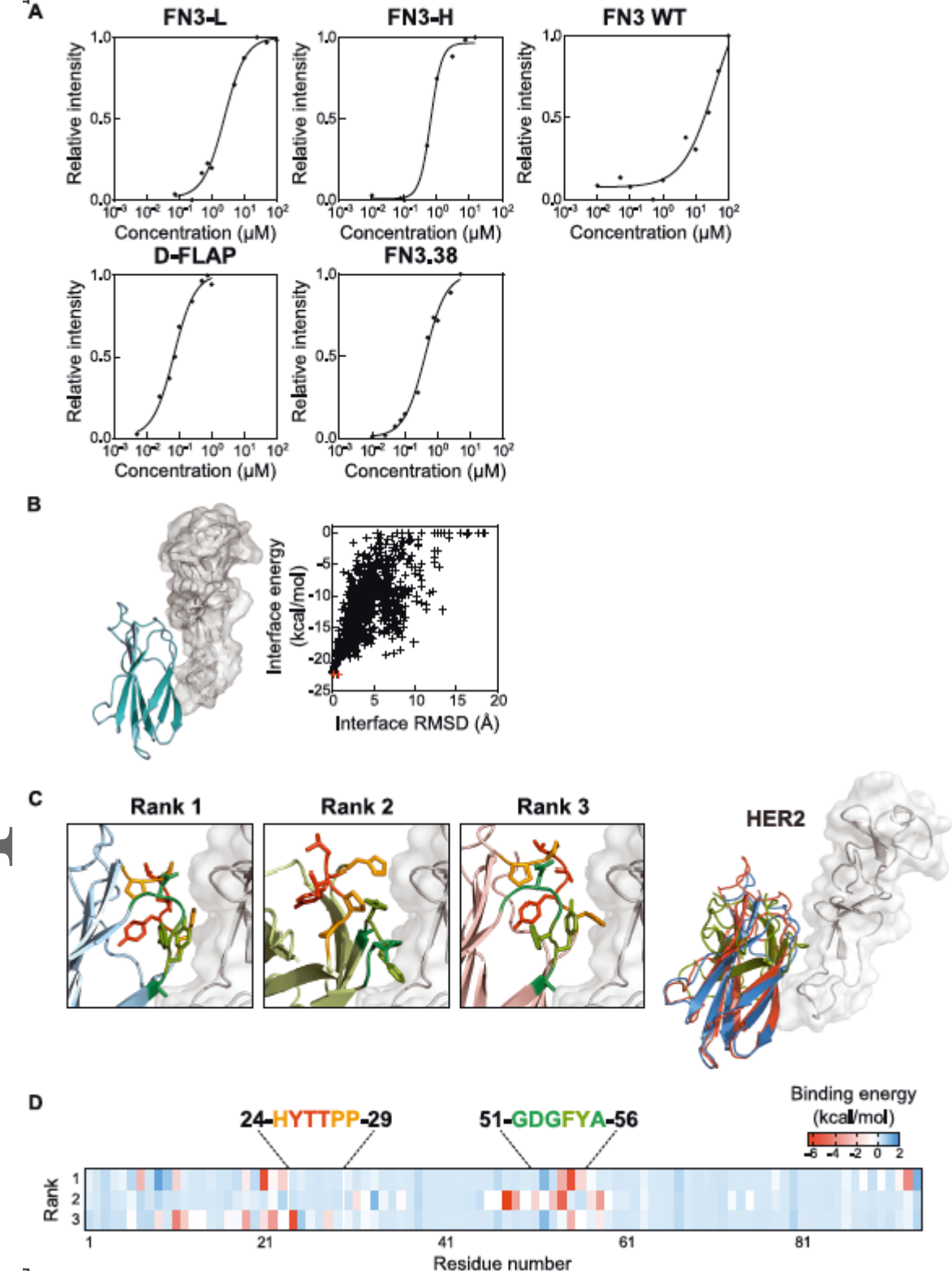
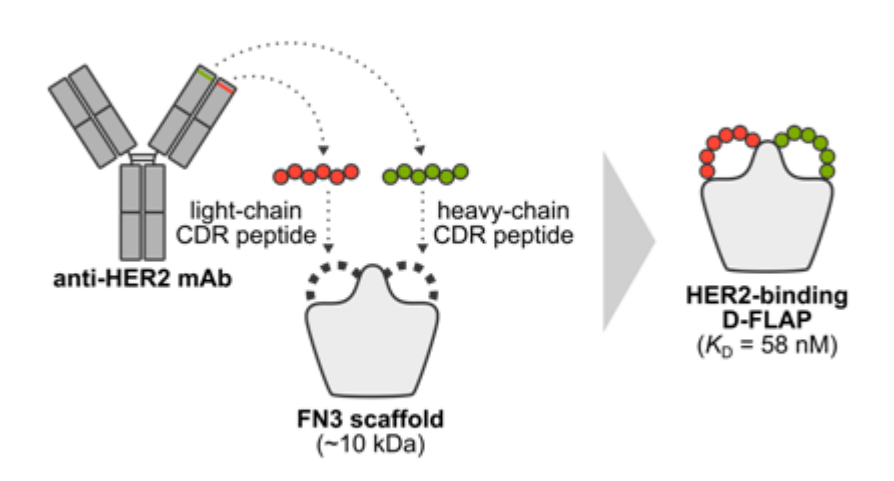


Figure 4. Evaluation of D-FLAP binding to HER2. A) Estimation of D-FLAP binding affinity to HER2 by ELISA. K_D values were estimated by curve fitting with non-linear regression. Representative data from three independent experiments are shown. B) Interface energy versus interface RMSD plot of the models obtained after local refinement docking of the lowest energy This article is protected by copyright. All rights reserved.

model from structural clustering analysis. The crosses in red indicate the three models with the lowest energy scores. The structure of the three models (Rank 1-3) and their position relative to HER2 are shown beside the plot. C) Structures of the three docking models with the lowest energy scores obtained after structural clustering analysis. The models are labeled according to their energy scores, with Rank 1 having the lowest score. The rightmost structure shows the three models superimposed relative to HER2. The CDR-derived peptides from the VL and VH regions are depicted by the stick representation. D) Binding energy of each D-FLAP residue to HER2 was calculated for the three docking models and shown as a heat map. The sequences and positions of the CDR-derived peptides are also indicated. C and D) The colors of the residues in the stick representation in C correspond to the residue letter colors in D: Orange and red represent the VL CDR-derived peptides, while turquoise and green represent the VH CDR-derived peptides, respectively. Red and green represent the initially identified HER2-binding residues from the VL and VH CDRs, respectively.



Target-binding small proteins are promising alternatives to monoclonal antibodies (mAbs). In this study, a computational strategy to design and screen D-FLAPs, which are mimetics bearing dual complementarity-determining region peptides derived from a mAb, is described. This strategy can be applied to various mAb drugs and allow the rational design of small protein alternatives.